

The Southern Galactic Plane Survey: Polarized Radio Continuum Observations and Analysis

M. Haverkorn¹², B. M. Gaensler³⁴
Harvard-Smithsonian Center for Astrophysics, 60 Garden Street, Cambridge MA 02138;
marijke@astro.berkeley.edu, bgaensler@cfa.harvard.edu

N. M. McClure-Griffiths
Australia Telescope National Facility, CSIRO, PO Box 76, Epping, NSW 1710, Australia;
naomi.mcclure-griffiths@csiro.au

J. M. Dickey
Physics Department, University of Tasmania, Private Bag 21, Hobart TAS 7001, Australia;
john.dickey@utas.edu.au

A. J. Green
School of Physics, University of Sydney, NSW 2006, Australia; agreen@physics.usyd.edu.au

ABSTRACT

The Southern Galactic Plane Survey (SGPS) is a radio survey in the 21 cm H I line and in 1.4 GHz full-polarization continuum, observed with the Australia Telescope Compact Array and the Parkes 64m single dish telescope. The survey spans a Galactic longitude of $253^\circ < l < 358^\circ$ and a latitude of $|b| < 1^\circ$ at a resolution of 100 arcsec and a sensitivity below 1 mJy/beam. This paper presents interferometer only polarized continuum survey data and describes the data taking, analysis processes and data products. The primary data products are the four Stokes parameters I, Q, U, and V in 25 overlapping fields of $5^\circ.5$ by 2° , from which polarized intensity, polarization angle and rotation measure are calculated. We describe the effects of missing short spacings, and discuss the importance of the polarized continuum data in the SGPS for studies of fluctuations and turbulence in the ionized interstellar medium and for studying the strength and structure of the Galactic magnetic field.

Subject headings: ISM: magnetic fields — H II regions — ISM: structure — techniques: polarimetric — radio continuum: ISM — turbulence

1. Introduction

Galactic magnetism is one of the major components in the Milky Way, mostly in equipartition with gas and cosmic rays. Interstellar magnetic fields are believed to profoundly influence the ionized interstellar medium (ISM) through flux freezing and energy dissipation, affect star formation, determine the trajectories and acceleration of low

and medium energy cosmic rays and play a major role in the turbulent gas dynamics (see e.g. reviews by Ferrière 2001, Scalo & Elmegreen 2004, Elmegreen & Scalo 2004).

Knowledge about the strength and structure of the Galactic magnetic field is still sketchy. Yet, the field has received increasing attention, not only with the objective of studying magnetic fields in galaxies but also because the Galactic magnetized ISM forms a polarized foreground which needs to be determined for Cosmic Microwave Background Polarization (de Oliveira-Costa et al. 2003) and Epoch of Reionization studies (Morales & Hewitt 2004).

The only methods to probe Galactic magnetic

¹Jansky Fellow, National Radio Astronomy Observatory

²Current address: Astronomy Department UC-Berkeley, 601 Campbell Hall, Berkeley CA 94720

³Alfred P. Sloan Fellow

⁴Current address: School of Physics A29, The University of Sydney, NSW 2006, Australia

fields in diffuse ionized gas over a large range of spatial scales are by way of radio polarization and Faraday rotation. Right and left circularly polarized components of radio emission experience birefringence while propagating through a magnetized and ionized medium. This causes the polarization angle of linearly polarized emission ϕ to rotate as a function of wavelength λ as $\Delta\phi = \text{RM}\lambda^2$, where the rotation measure RM is $\text{RM} = 0.81 \int n_e \mathbf{B} \cdot d\mathbf{s}$, n_e is the thermal electron density in cm^{-3} , \mathbf{B} is the magnetic field vector in microGauss, $d\mathbf{s}$ is the path length vector through the medium in parsecs, and the integral is along the line of sight from the observer to the source of polarized emission. Therefore, Faraday rotation measurements allow estimation of the magnetic field component along the line of sight, weighted by the electron density, and integrated over the pathlength. Depolarization characteristics can be used to determine the scale and amplitude of fluctuations in the medium.

The observed polarized radiation used to trace the Galactic magnetic field can come from pulsars, polarized extragalactic sources or diffuse Galactic synchrotron emission (including supernova remnants). All of these sources have their own advantages and disadvantages. Pulsars are unique because model-dependant distance estimates allow constraining of the path length, and because a dispersion measure can be calculated, which in combination with RM yields a direct measure of the magnetic field averaged over the path length. However, they are scarce and distributed mainly in the Galactic plane. Unresolved extragalactic sources, on the other hand, are distributed all over the sky. But they have an intrinsic RM contribution, and currently published datasets yield an average of one source deg^{-2} in the Galactic plane (Brown et al. 2003, Brown et al., in prep), and only 0.02-0.03 source deg^{-2} in the rest of the sky (e.g. Simard-Normandin et al. 1981, Broten et al. 1988). Only diffuse synchrotron emission provides a pervasive background of polarized radiation which can be used to form RM maps of large fields in the sky with high resolution (Haverkorn et al. 2003a,b; Uyaniker et al. 2003; Reid 2004). Diffuse synchrotron emission does suffer from depolarization, which decreases the possible measurements of RM, but which in itself can yield information about the fluctuations in the magneto-ionized interstellar medium (Gaensler et al. 2001).

Recently the whole sky has been mapped in absolutely calibrated polarized continuum at 1.4 GHz (see Wolleben et al. 2005 for the Northern sky, and Testori et al. 2004 in the South) at a resolution of about half a degree. More than half of the Galactic plane is being surveyed at the much higher resolution of an arcmin, in two separate polarization surveys. The Canadian Galactic Plane Survey (CGPS, Taylor et al. 2003) covers the Northern Sky at Galactic longitudes $74.2^\circ < l < 147.3^\circ$ and latitudes $-3.6^\circ < b < +5.6^\circ$. The Southern Galactic Plane Survey (SGPS, McClure-Griffiths et al. 2005; hereafter Paper I) extends from $253^\circ < l < 358^\circ$ (Phase I) and $5^\circ < l < 20^\circ$ (Phase II) at longitudes $|b| < 1^\circ$. In both these projects full-polarization continuum and H I were observed simultaneously. Although for the H I part of the SGPS data from the Australia Telescope Compact Array (ATCA) interferometer and Parkes 64-m single dish have been combined, the polarization measurements discussed here are derived from ATCA observations only.

The H I data in the SGPS have been discussed in detail in Paper I, whereas a test region covering the region $325^\circ.5 < l < 333^\circ.5$ and $-0^\circ.5 < b < +3^\circ.5$ is described in Gaensler et al. (2001) and McClure-Griffiths et al. (2001). This paper describes the radio continuum data of the SGPS Phase I, i.e. at Galactic longitudes $253^\circ < l < 358^\circ$ (hereafter referred to as SGPS); the continuum data observed in the region $5^\circ < l < 20^\circ$ will be discussed elsewhere. In Sect. 2 we briefly summarize some details about the telescopes, data taking, and calibration. Furthermore, this Section describes the polarization calibration and the effect of missing short spacings. In Section 3 we present the data, and Sect. 4 discusses some of the science done with the polarized SGPS data.

2. The Survey

2.1. Observations

The ATCA is a radio interferometer near Narrabri, NSW, Australia, consisting of six 22m-diameter dishes. Five of these are located on a 3km long east-west track, or a 200m north-south track, while the sixth element is fixed 3km west of the east-west track, so that baselines from 31m to 6km can be achieved. The SGPS was observed

Source	RA (h:m:s) (J2000.0)	dec (°:m:s) (J2000.0)	l (°)	b (°)	I _{1.4} (Jy)	no. pointings	time (hr)
PKS 0857-43	08:59:28	-43:45:44	265.15	+1.45	26	7	1.7
CTB 31	08:59:07	-47:31:24	267.95	-1.06	100	7	1.7
PKS 0922-51	09:24:26	-51:59:34	274.01	-1.15	12	6	1.7
GAL 282.0-01.2	10:06:38	-57:12:11	282.02	-1.18	11	7	1.7
Gum 29	10:24:15	-57:46:58	284.31	-0.33	73	7	1.7
GAL 285.3-00.0	10:31:29	-58:02:08	285.26	-0.05	12	7	1.5
NGC 3372	10:44:19	-59:37:34	287.61	-0.85	158	7	1.5
NGC 3581	11:11:57	-61:18:49	291.28	-0.71	37	}10	}2.1
GRS 291.6-00.5	11:15:10	-61:16:45	291.63	-0.54	22		
GAL 298.2-00.3	12:10:03	-62:50:00	298.23	-0.34	16	}13	}3.0
GAL 298.9-00.4	12:15:26	-63:01:28	298.86	-0.44	15		
GAL 305.4+00.2	13:12:33	-62:34:43	305.36	+0.19	18	10	2.4
GRS 307.1+01.2	13:26:19	-61:23:01	307.10	+1.21	10	7	1.7
GAL 309.6+00.1	13:46:49	-60:24:29	309.72	+1.73	119	7	1.7
GAL 316.8-00.1	14:45:19	-59:49:32	316.80	-0.06	25	7	1.7
GAL 327.3-00.5	15:52:35	-54:38:00	327.30	-0.56	31	7	1.5
GRS 326.7+00.6	15:44:48	-54:06:42	326.66	+0.57	21	7	1.5
GAL 331.5-00.0	16:12:03	-51:26:55	331.52	-0.07	25	7	1.5
GRS 333.6-00.2	16:22:10	-50:06:07	333.60	-0.22	38	7	1.4

Table 1: Additional observations to increase SGPS dynamic range around bright sources. From left to right, the columns denote the source’s name, its coordinates in RA and dec, its Galactic longitude and latitude, its integrated flux density at 1.4 GHz, the number of pointings and the total amount of time spent observing this source.

only on east-west baselines, between 1998 December and 2001 June. As the main objective of the SGPS is measuring diffuse emission, we exploited the compact configurations of the instrument. The 6km antenna was excluded and five different compact configurations were used to ensure continuous uv-coverage at baselines from approximately 31m to 3km, which results in a resolution of ~ 80 arcsec (smoothed to 100 arcsec for all fields) and sensitivity up to scales of about 30 arcmin.

The ATCA data signal is processed through two intermediate frequency (IF) channels, allowing observations in the H I band and a continuum band simultaneously. Data in the continuum band were averaged into 12 frequency channels of each 8 MHz wide, centered on 1336 MHz to 1432 MHz, where the 1408 MHz band was flagged due to internal interference. Two feeds X and Y detect orthogonal linear polarizations, which are correlated into signals in four channels XX , YY , XY and YX

for each antenna pair. These were translated into Stokes parameters I, Q, U, and V (Hamaker & Bregman 1996).

The SGPS data are divided into fields of $5^\circ.5$ in Galactic longitude and 2° in Galactic latitude, centered on $b = 0^\circ$, and slightly overlapping in longitude. The central longitudes of the fields run from 255° to 355° in steps of 5° . Each field consists of 105 pointings in a hexagonal pattern with Nyquist spacing of $19'$ between pointing centers. This results in a constant gain across fields except at the edges of the survey, and decreases the contribution of instrumental polarization to about 0.1%. Each pointing was observed for 30 sec before continuing to the next pointing, circling through a field for 12 hours. Multiple 12-hour runs assured regular uv-coverage and a total observing time per pointing of at least 20 min. See Paper I for observational details about the SGPS data set such as exact locations and sizes of the fields and point-

ings, uv-coverage etc.

Calibration, deconvolution and flagging eliminated most artifacts in the field. However, grating rings with a radius of 0.8° can still be seen around bright and extended sources, mostly in total intensity but occasionally also in polarization, sometimes accompanied by spokes. This is due to the regular spacing of about 15m in the telescope configurations of the east-west array, combined with the relatively low dynamic range of the SGPS of approximately 150:1 (see Paper I). The bright sources and/or their artifacts can induce instrumental polarization if strong enough. To mitigate these artifacts, we took additional observations of strong and extended sources in or near the field of observation which increased the dynamic range in these pointings. These sources were observed in small mosaics with the same spacing, pattern and approximate observing time as the pointings in the SGPS, as detailed in Table 1. The noise in the final Q, U images is ~ 0.3 mJy/beam at low Galactic longitudes, and increases to ~ 0.6 mJy/beam towards the Galactic Center. The average error in polarization angle on the total band is 3° , the average error in angle in one 8 HMz channel is 10° .

The data were reduced using the software package MIRIAD (Sault & Killeen 2003). Flux and bandpass variations between antennas were calibrated using the primary calibrator PKS B1934-638, assuming a flux of 14.9 Jy at 1.4 GHz (Reynolds 1994). The primary calibrator was observed for ~ 10 min at the beginning and end of each observing session. For each program field, a secondary calibrator close to the field was observed. Atmospheric gain and delay variations could be monitored and calibrated using the secondary calibrators. For some fields the secondary calibrator was observed regularly during the night so that sufficient hour angle coverage could be obtained and the calibrator's intrinsic polarization could be separated from the instrumental polarization leakage. For the remaining fields the hour angle range of the secondary calibrator was too small to obtain polarization calibration so that 1934-628 was used instead, assuming it is unpolarized at 1.4 GHz. These leakage and gain parameters per antenna, combined with the bandpass calibrations from the primary calibrator, were propagated to the program fields. Additional flagging per pointing and/or per Stokes parameter was necessary

to eliminate bad data due to interference. For details about the calibrators and non-polarization calibration, see Paper I.

The pointings were linearly combined for each 11 deg^2 field and imaged jointly using a standard grid-and-FFT scheme. Superuniform weighting was used for maximum reduction of grating rings, at the expense of signal-to-noise. The maps were deconvolved jointly, which allows some of the missing large-scale structure to be retrieved (Sault et al. 1996). Using a maximum entropy algorithm (Narayan & Nityananda 1984), the Stokes parameters can be deconvolved jointly (routine PMOSMEM in MIRIAD) or separately (MOSMEM). As has been noted by Sault et al. (1999) and confirmed with the SGPS data, for diffuse polarization mostly uncorrelated to total intensity joint deconvolution is mildly inferior to separate deconvolution. A deconvolution algorithm for mosaics based on Steer CLEANing (MOSSDI, Steer et al. 1984) did not give significantly better results, therefore maximum entropy deconvolution for all Stokes parameters separately was used. The images were restored with a Gaussian beam of 100 arcsec resolution.

2.2. Missing short spacings

An interferometer is insensitive to structure on large scales due to a finite minimum spacing between dishes. Therefore, the SGPS does not contain structure on scales larger than about 30 arcmin.

Missing large-scale structure in Stokes Q and U can destroy or create small scale structure in polarized intensity (Haverkorn et al. 2004a), i.e. enhancements in polarization on small scales can become depressions if zero spacing data is added, or vice versa. Furthermore, due to the non-linear dependence of polarization angle on Stokes Q and U, the linear relation between polarization angle and wavelength squared caused by Faraday rotation may be destroyed, although this is not always the case. Specifically, if the large scale emission is much stronger than the small scale emission, the computed RM will deviate from the true value. Therefore, addition of single-dish structure (Stanimirović 2002) to polarized emission from interferometers is imperative (Uyaniker et al. 1998).

Although we plan to eventually include single-

dish polarization data from the Parkes 64m telescope in the SGPS, the polarization data discussed in this paper do not contain large-scale structure. This introduces important caveats associated with the use of these data, as we now discuss.

Spatial RM variations on scales smaller than the sensitivity scale of the interferometer ($< 0.5^\circ$) cause a spread in polarization angle within the field of view. If the RM variations are large enough to cause a variation in polarization angle which is higher than about $\pi/2$ radians, this will effectively randomize Q and U within the field of view, destroying any large-scale structure in Q and U (Haverkorn et al. 2004a). Therefore, an interferometer can detect all of the Q and U structure if RM variations within its field of view are large enough. In the case of the ATCA, RM variations of about 40 rad m^{-2} or larger on scales smaller than the field of view cause a sufficiently large spread in polarization angle that Q and U are effectively randomized over the field of view, so that no large-scale structure in Q and U remains (even though large-scale structure in RM is present). The observed value of RM variations is similar to this critical value.

Radiation from unresolved extragalactic point sources and pulsars does not have a large-scale component. Any contribution from diffuse foreground emission to the polarized emission in the direction of the point source can be estimated and subtracted using the source's immediate surroundings (Brown et al. 2003). Therefore, missing large-scale structure will not influence polarized point source measurements.

Care has to be taken in interpretation of the diffuse emission. For structures that emit on small scales detectable by the interferometer (e.g. the Vela supernova remnant) it can be assumed that the RM measured from the emitting structures is accurate. However, for structures produced by pure Faraday rotation it is not certain whether the computed RM is equal to the real RM. For most pixels no linear fit between ϕ and λ^2 could be found, indicating depolarization and/or missing large-scale structure. Only for a small fraction of the SGPS data (typically a few percent) the calculated linear fit for ϕ against λ^2 yields a reduced $\chi^2 < 2$ and a signal-to-noise > 5 . Where this structure does not coincide with small-scale emission, RMs may deviate from the true values.

However, even where large-scale polarized structure is missing the SGPS can be used as a detection survey. The polarization data contain a variety of 'objects' that are invisible in total intensity and unrelated to emission at any other wavelength. These polarized objects can be followed up with single-dish observations to measure their large-scale emission, which will allow detailed study.

3. Results

The resulting primary data products from the ATCA are maps of Stokes I, Q, U and V, from which debiased polarized intensity P and polarization angle ϕ are constructed as

$$P = \sqrt{Q^2 + U^2 - \sigma^2} \quad (1)$$

$$\phi = 0.5 \arctan \frac{U}{Q} \quad (2)$$

(Wardle & Kronberg 1974) where σ is the rms noise in the Q and U maps, computed as the standard deviation of Stokes V.

Total intensity Stokes I, Stokes Q, Stokes U and polarized intensity P maps for the complete SGPS are shown in Fig. 1. For the first field shown, Stokes V is added for illustration purposes. Some polarization coinciding with strong sources in total intensity is artificial and caused by instrumental polarization, down to a level of 0.1%. The strongest artifacts are marked with circles in Fig. 1. The remaining extended structure is believed to be real, and the lack of correlation with total intensity indicates that the fluctuations in polarized emission are due to depolarization and Faraday rotation effects.

In a large part of the maps there is small-scale total intensity but no polarized emission, indicating that the synchrotron radiation is completely depolarized due to the abundant small-scale structure in magnetic field and/or electron density in the inner Galactic plane. Depolarization due to structure in electron density is evidenced by an anticorrelation between polarization and H α emission frequently observed in the SGPS, see Fig. 2.

From the polarization angle maps at 12 frequencies, rotation measure RM can be computed as $\phi = \text{RM}\lambda^2$, an example of which is shown in Fig. 3. This can be done using all 12 frequency channels

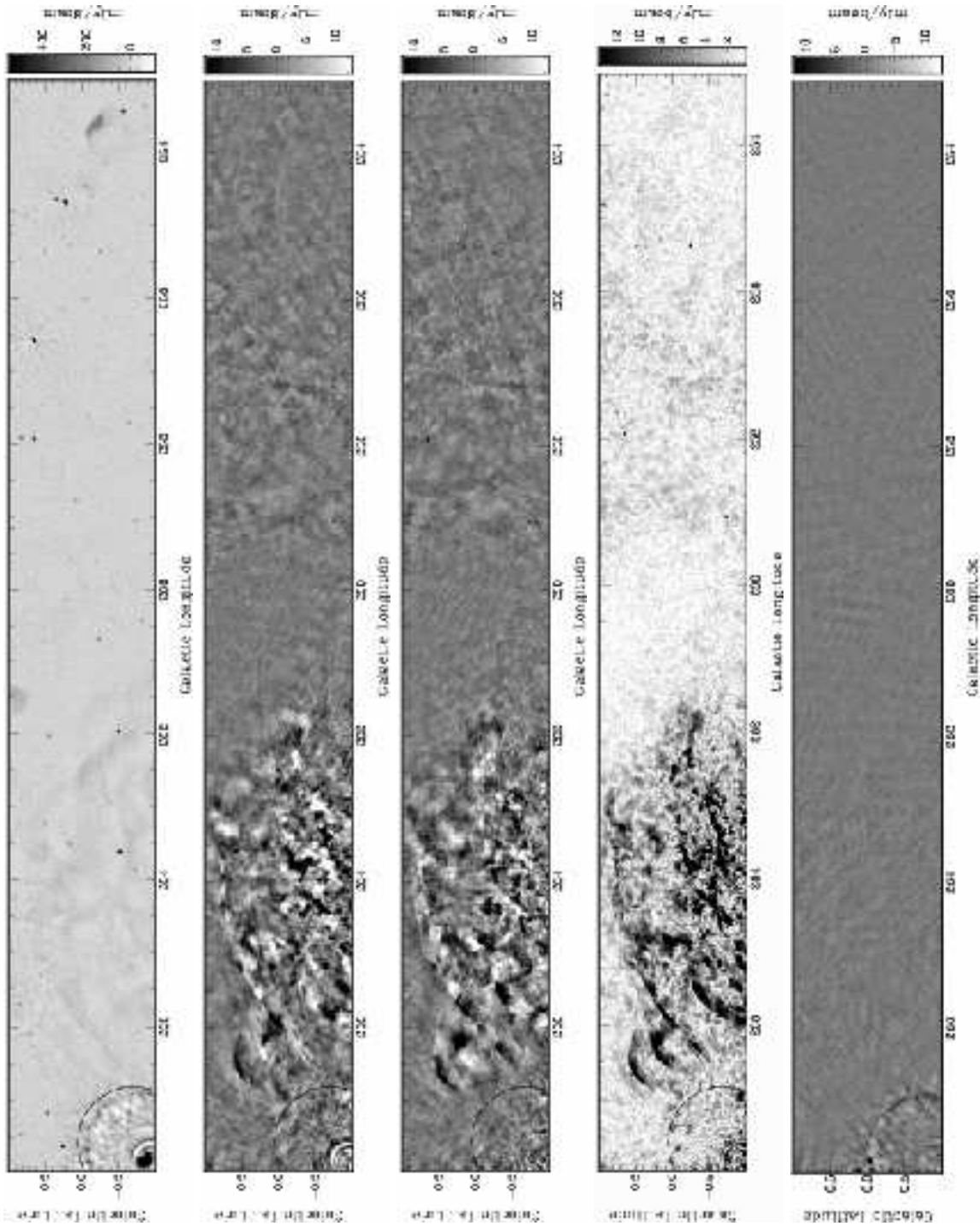


Fig. 1.— The Southern Galactic Plane Survey total intensity Stokes I, Stokes Q, Stokes U and polarized intensity P from top to bottom. On the first page only a Stokes V map has been added to the bottom. Overlaid circles denote artifacts in the data due to the regular 15m spacing of the ATCA, and no large-scale structure ($> 0.5^\circ$) is included. The top half of a weak shell centered at $l \approx 264^\circ$ is the Vela supernova remnant.

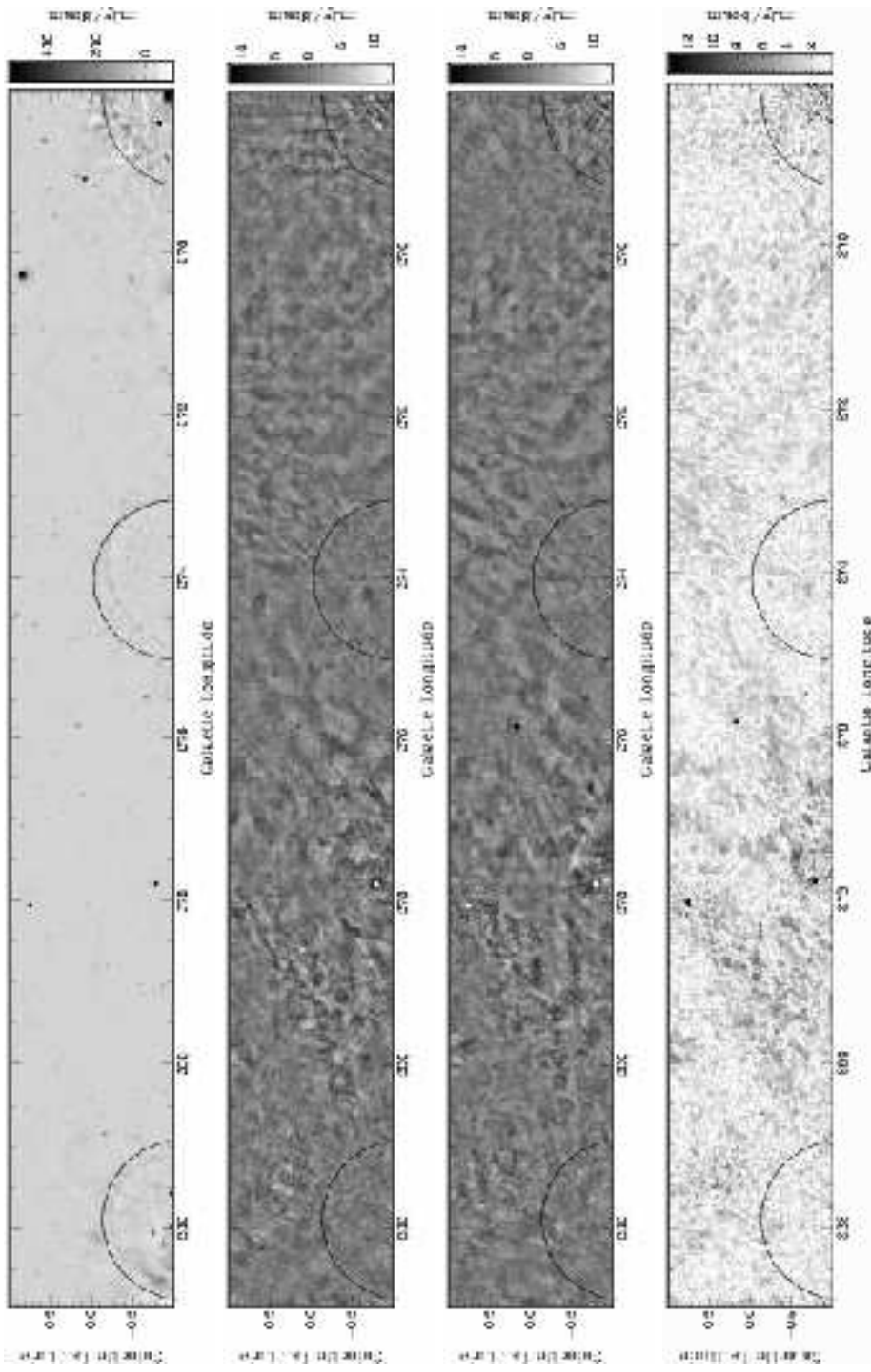


Fig. 1.— — continued.

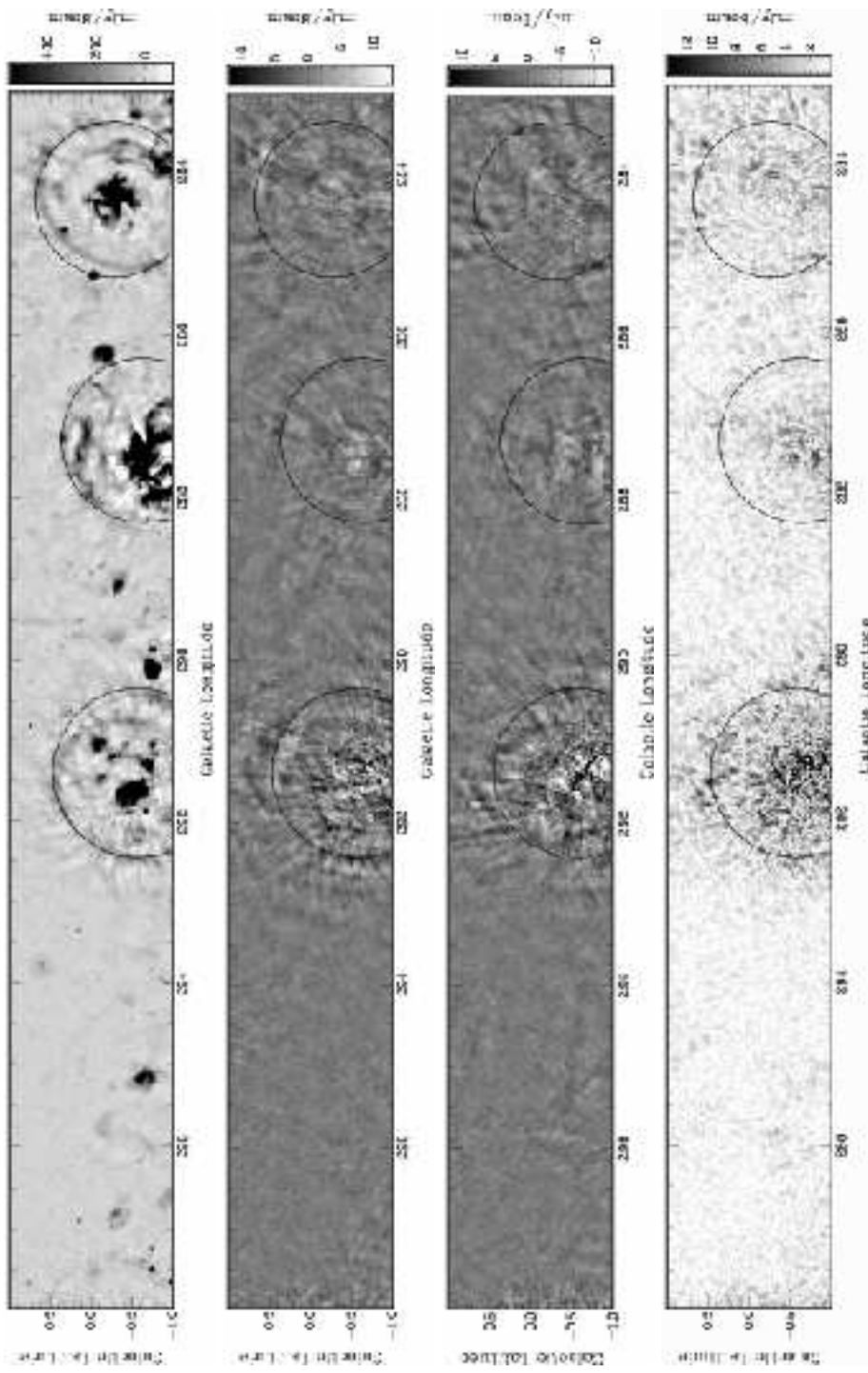


Fig. 1.— — continued.

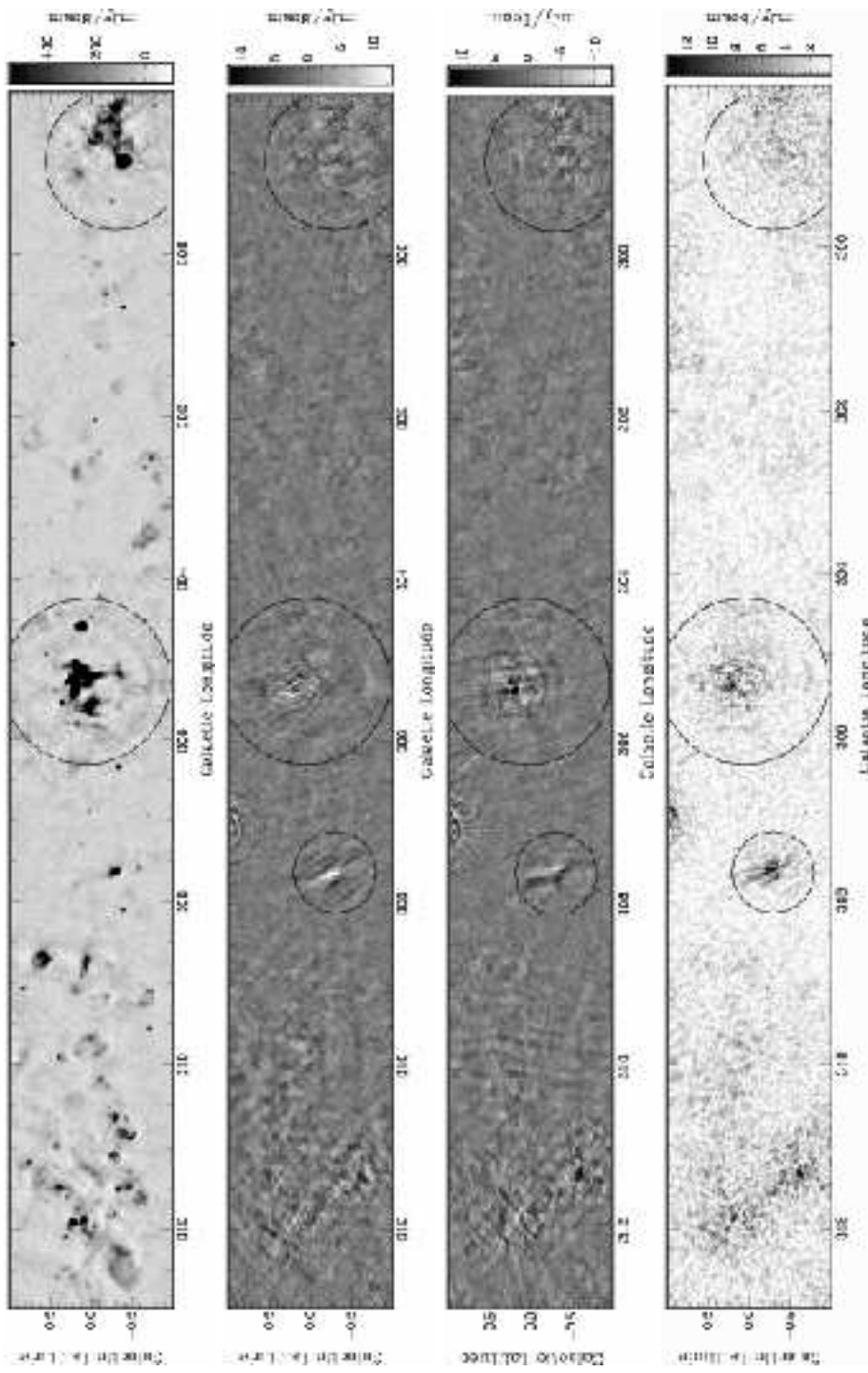


Fig. 1. — continued.

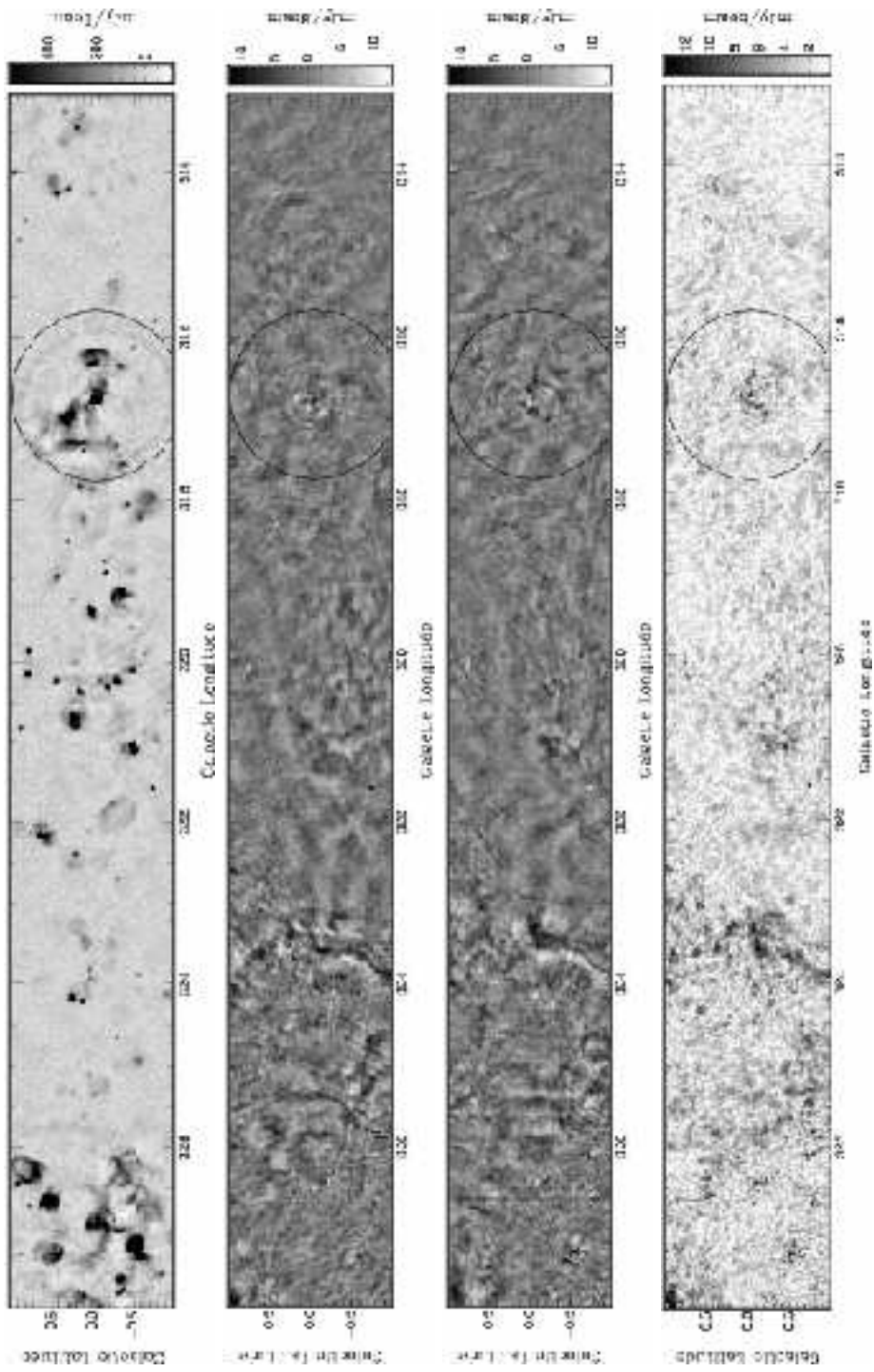


Fig. 1.— — continued.

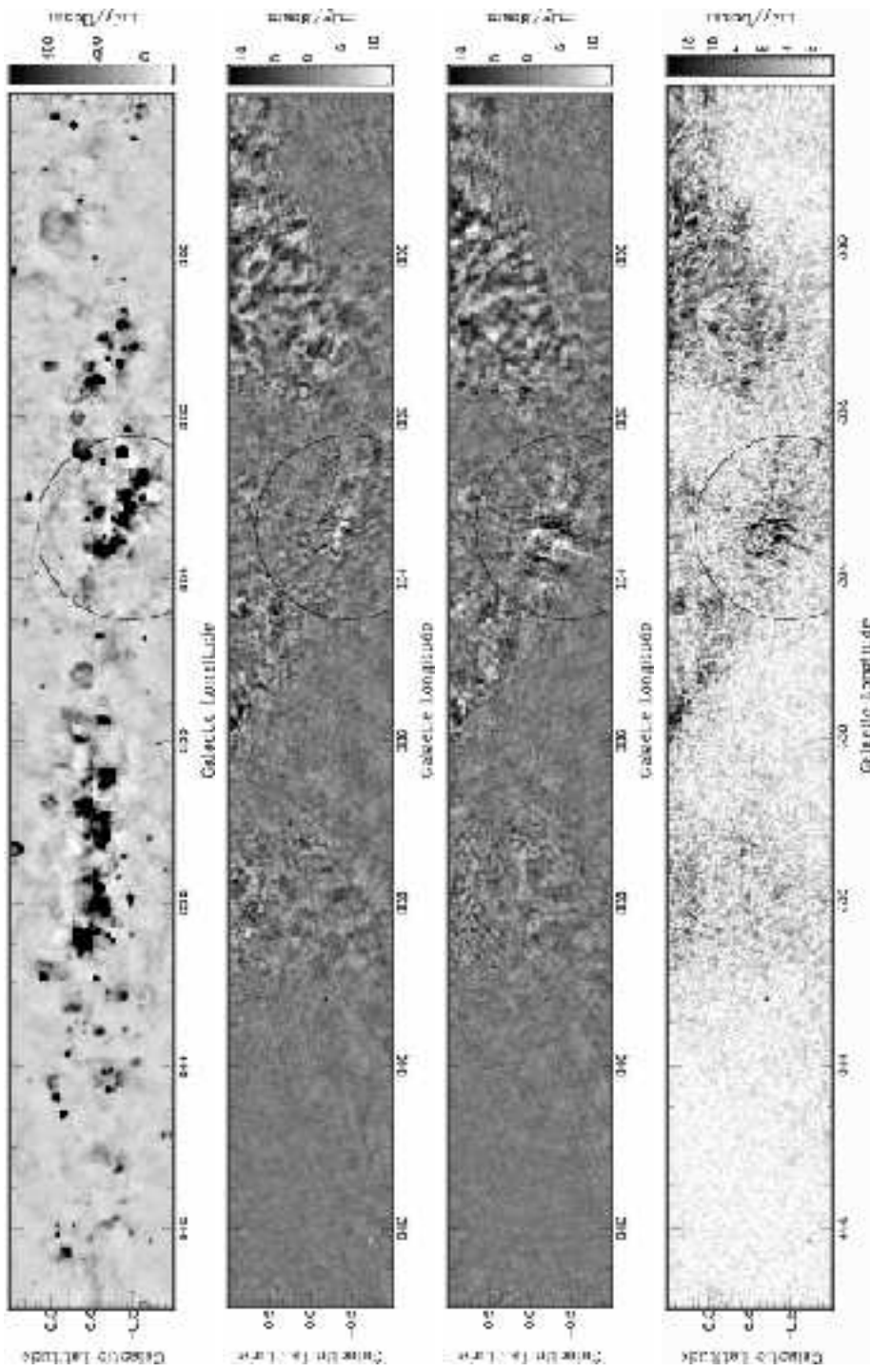


Fig. 1.— — continued.

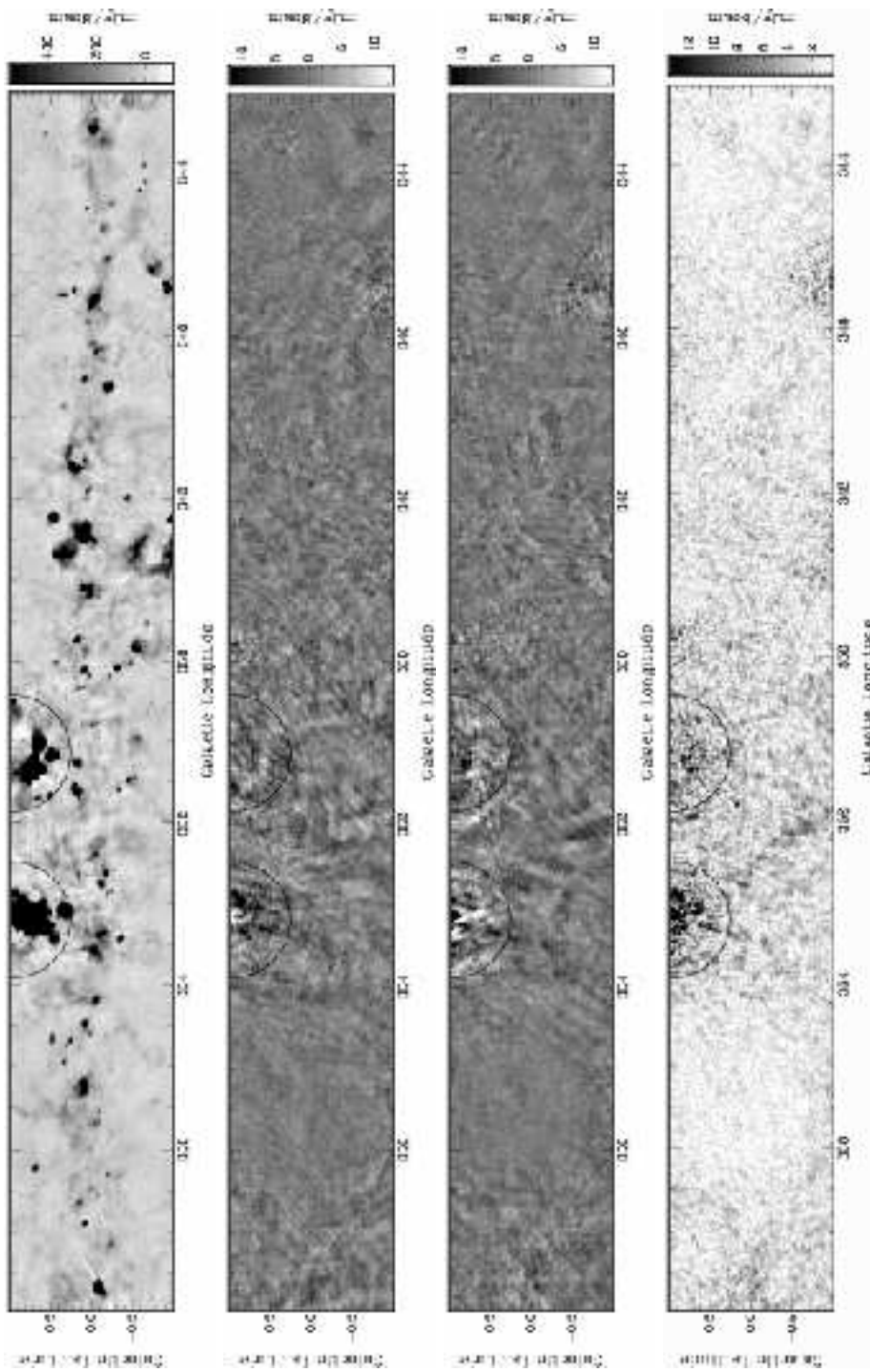


Fig. 1.— — continued.

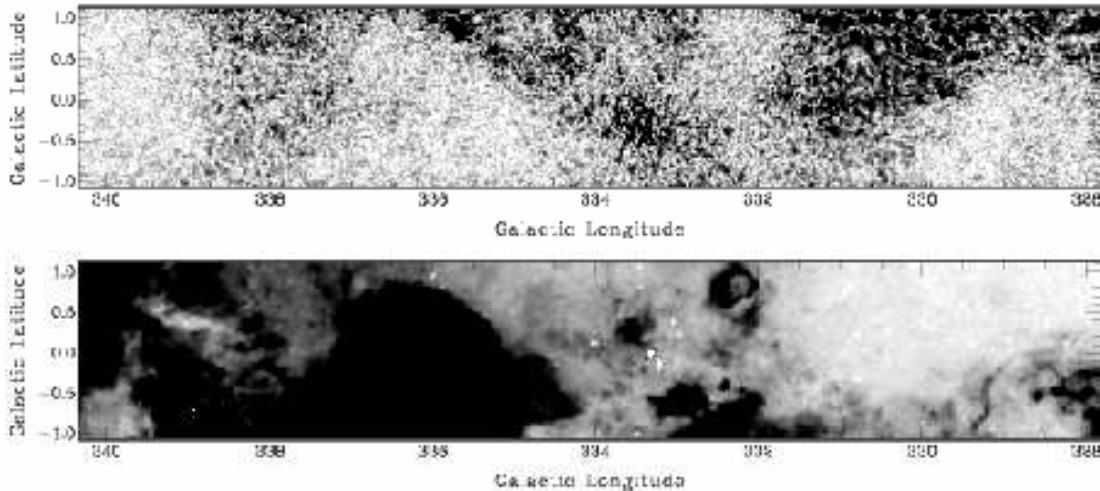


Fig. 2.— Anticorrelation between SGPS polarized intensity (top) and $H\alpha$ emission from the SHASSA survey (bottom). The circle denotes artifacts in the polarization data. High $H\alpha$ intensity is saturated to show the weak emission better.

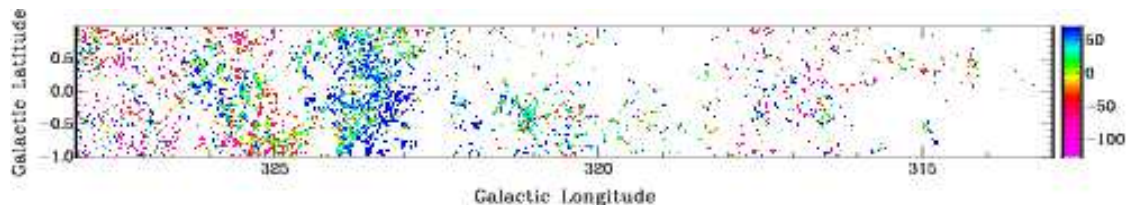


Fig. 3.— Example of the SGPS RM data, obtained with the PACERMAN algorithm (Dolag et al. 2005; Vogt et al. 2005).

separately, or averaging them into 3 wider frequency bands, for which the average error in the polarization angle is $\sim 3^\circ$, which give similar results. RM has been calculated using the algorithm PACERMAN (Dolag et al. 2005; Vogt et al. 2005), which computes RM values not only taking into account the π rad ambiguity of polarization angle, but also consistency with the surrounding pixels. The results obtained with the PACERMAN algorithm were checked against maps obtained by simple pixel-by-pixel linear fits of ϕ against λ^2 . The results are very similar, although the PACERMAN maps look smoother than the pixel-by-pixel maps, and have slightly more pixels for which RM could be calculated.

3.1. Available data products

Maps of Stokes I, Q and U are available from the SGPS Data Server⁵, consisting of all 12 frequency channels averaged into one map. Data in individual frequency channels and rotation measure information are available upon request.

4. Science with the SGPS

From the SGPS test region, Gaensler et al. (2001) showed that the brightest polarized region originated in the Crux spiral arm at a distance of ~ 3.5 kpc, and was Faraday rotated by the ionized medium along its path length. Furthermore, they showed that voids in polarization are due to foreground H II regions with magnetic fields disordered on scales of ~ 0.2 pc, and found a depo-

⁵<http://www.atnf.csiro.au/research/HI/sgps/queryForm.html>

larization halo around the H II region RCW 94.

Using the RMs from the SGPS test region, Haverkorn et al. (2004b) concluded that a dominant source of fluctuations with an outer scale of a few parsecs exists in the spiral arms only, and suggested the structure could be caused by H II regions in the arms. This assertion was confirmed by statistical analysis of RMs of SGPS extragalactic point sources in the whole SGPS (Haverkorn et al. 2006a), which describes the detection of fluctuations with an outer scale smaller than ~ 17 pc in the Carina and Crux spiral arms, but not present in the interarm regions.

RM data from pulsars and polarized extragalactic point sources in the SGPS, combined with other available point source data, are being used to construct a model of the large-scale Galactic magnetic field (Haverkorn et al. 2006b, Brown et al., in prep), discussing the strength of the regular magnetic field and the abundance and locations of magnetic field reversals.

The SGPS is an excellent source for finding correlations between radio (de-)polarization and H II regions or molecular clouds, which indicate Faraday rotation effects due to photodissociation regions (PDRs) around H II regions (Gaensler et al. 2001; Wolleben & Reich 2004).

Finally, SGPS RM maps reveal individual objects that cannot be detected in any other way, such as the partial shell centered on $l = 278.5^\circ$. These objects do not show any correlation with $H\alpha$ measurements, indicating that the RM structure cannot be due to enhanced electron density. Therefore, these objects are likely purely magnetic, and not detectable otherwise.

5. Summary and conclusions

The polarized radio continuum part of the Southern Galactic Plane Survey (SGPS) provides a major new resource for studies of the ionized interstellar medium and Galactic magnetic field. The SGPS covers almost one third of the Galactic plane with a Galactic longitude coverage of $253^\circ < l < 358^\circ$, at Galactic latitudes $|b| < 1^\circ$. The rms sensitivity of the SGPS continuum data is ~ 0.3 mJy/beam increasing to double that number close to the Galactic Center, the instrumental polarization is below 0.1% and the resolution is $100''$. Due to beam depolarization at low reso-

lutions, maps with this high resolution reveal a wealth of polarization structure which would be depolarized in low resolution maps.

The polarized radio continuum data in the SGPS are uniquely suited for studies of the ionized gas and magnetic field strength and structure in the inner Galactic plane, taking into account the constraints of missing large-scale structure. The polarized intensity can be used for depolarization studies to obtain the scale of fluctuations in the magneto-ionized medium. Rotation measure data give information about the electron-density-weighted magnetic field strength along the line of sight, and can be used for statistical analysis of these fluctuations, large-scale modeling of the Galactic magnetic field, or study of individual magnetic objects.

The ATCA is part of the Australia Telescope, which is funded by the Commonwealth of Australia for operation as a National Facility managed by CSIRO. This research was supported by the National Science Foundation through grants AST-0307358 to Harvard College Observatory and AST-9732695 and AST-0307603 to the University of Minnesota. M.H. acknowledges support from the National Radio Astronomy Observatory (NRAO), which is operated by Associated Universities Inc., under cooperative agreement with the National Science Foundation. B.M.G. is supported by an Alfred P. Sloan Research Fellowship. We would like to thank J. Gelfand for help with observing, and the staff of the Australia Telescope National Facility for their support of this project, especially R. Haynes, D. McConnell, R. Sault, R. Wark, and M. Wieringa.

Facilities: ATCA.

REFERENCES

- Broten, N. W., MacLeod, J. M., & Vallee, J. P. 1988, *Ap&SS*, 141, 303
- Brown, J. C., Taylor, A. R., & Jackel, B. J. 2003, *ApJS*, 145, 213
- de Oliveira-Costa, A., Tegmark, M., O'Dell, C., Keating, B., Timbie, P., Efstathiou, G., & Smoot, G. 2003, *PhRvD*, 68, 8
- Dolag, K., Vogt, C., & Ensslin, T. A. 2005, *MNRAS*, 358, 726

- Elmegreen, B. G., & Scalo, J. 2004, *ARA&A*, 42, 211
- Ferrière, K. M. 2001, *RvMP*, 73, 1031
- Gaensler, B. M., Dickey, J. M., McClure-Griffiths, N. M., Green, A. J., Wieringa, M. H., Haynes, R. F. 2001, *ApJ*, 549, 959
- Hamaker, J. P., & Bregman, J. D. 1996, *A&AS*, 117, 161
- Haverkorn, M., Katgert, P., de Bruyn, A. G. 2003a, *A&A*, 403, 1031
- Haverkorn, M., Katgert, P., & de Bruyn, A. G. 2003b, *A&A*, 404, 233
- Haverkorn, M., Katgert, P., & de Bruyn, A. G. 2004a, *A&A*, 427, 549
- Haverkorn, M., Gaensler, B. M., McClure-Griffiths, N. M., Dickey, J. M., & Green, A. J. 2004b, *ApJ*, 609, 776
- Haverkorn, M., Brown, J. C., Gaensler, B. M., McClure-Griffiths, N. M., Dickey, J. M., & Green, A. J. 2006, *ApJL*, 637, 33
- Haverkorn, M., Gaensler, B. M., Brown, J. C., McClure-Griffiths, N. M., Dickey, J. M., & Green, A. J. 2006, *Ast. Nach.*, in press
- McClure-Griffiths, N. M., Dickey, J. M., Gaensler, B. M., Green, A. J., Haverkorn, M., Strasser, S. 2005, *ApJS*, 158, 178 (Paper I)
- McClure-Griffiths, N. M., Green, A. J., Dickey, J. M., Gaensler, B. M., Haynes, R. F., & Wieringa, M. H. 2001, *ApJ*, 551, 394
- Morales, M. F., & Hewitt, J. 2004 *ApJ*, 615, 7
- Narayan, R., & Nityananda, R. 1986, *ARA&A*, 24, 127
- Reid, R. 2004, in *The Magnetized Interstellar Medium*, ed. B. Uyaniker, W. Reich, R. Wielebinski (Katlenburg-Lindau: Copernicus GmbH), 39
- Reynolds, J. E. 1994, *ATNF Technical Document Series*, Tech. Rep. AT/39.3/0400 (Sydney: Australia Telescope National Facility)
- Sault, R. J., Bock, D. C.-J., & Duncan, A. R. 1999, *A&AS*, 139, 387
- Sault, R. J., & Killeen, N. E. B. 2003, *The Miriad User's Guide* (Sydney: Australia Telescope National Facility)
- Sault, R. J., Staveley-Smith, L., & Brouw, W. N. 1996, *A&AS*, 120, 375
- Scalo, J., & Elmegreen, B. G. 2004, *ARA&A*, 42, 275
- Simard-Normandin, M., Kronberg, P. P., & Button, S. 1981, *ApJS*, 45, 97
- Stanimirović, S. 2002, in *ASP Conference Proceedings*, Vol. 278, eds. S. Stanimirović, D. Altschuler, P. Goldsmith, and C. Salter, (San Francisco: Astronomical Society of the Pacific) p. 375-396
- Steer, D. G., Dewdney, P. E., & Ito, M. R. 1984, *A&A*, 137, 159
- Taylor, A. R., Gibson, S. J., Peracaula M., Martin, P. G., Landecker, T. L., Brunt, C. M., Dewdney, P. E., Dougherty, S. M., Gray, A. D., Higgs, L. A., Kerton, C. R., Knee, L. B. G., Kothes, R., Purton, C. R., Uyaniker, B., Wallace, B. J., Willis, A. G., & Durand, D. 2003, *AJ*, 125, 3145
- Testori, J. C., Reich, P., & Reich, W. 2004, in *The Magnetized Interstellar Medium*, ed. B. Uyaniker, W. Reich, R. Wielebinski (Katlenburg-Lindau: Copernicus GmbH), 57
- Uyaniker, B., Fürst, E., Reich, W., Reich, P., & Wielebinski, R. 1998, *A&AS*, 132, 401
- Uyaniker, B., Landecker, T. L., Gray, A. D., & Kothes, R. 2003, *ApJ*, 585, 785
- Vogt, C., Dolag, K., & Ensslin, T. A. 2005, *MNRAS*, 358, 732
- Wardle, J. F. C., & Kronberg, P. P. 1974, *ApJ*, 194, 249
- Wolleben, M., Landecker, T. L., Reich, W., & Wielebinski, R., 2005, *A&A*, in press, astro-ph/0510456
- Wolleben, M., & Reich, W. 2004, *A&A*, 427, 537